CINTAL - Centro de Investigação Tecnológica do Algarve
Universidade do Algarve

A simple detector for passive acoustic monitoring of ocean noise

S.M. Jesus

Rel 04/19 - CINTAL
26/December/2019

Universidade do Algarve
Campus de Gambelas
8005-139 Faro
Portugal

tel: +351-289244422
fax: +351-289864258
cintal@ualg.pt
www.cintal.ualg.pt

	CINTAL Universidade do Algarve, Campus de Gambelas, 8005-139 Faro, Portugal tel: +351-289244422 Fax: +351-289864258, cintal@ualg.pt, www.cintal.ualg.pt
Laboratory that performed the work	SiPLAB, FCT, Universidade do Algarve, Campus de Gambelas, 8005-139 Faro, Portugal tel: +351289800949
Project	SUBECO
Title	A simple detector for passive acoustic monitoring of ocean noise
Author	S.M. Jesus
Date	December 26, 2019
Reference	04/19 - CINTAL
Number of pages	25 (twenty five)
Abstract	This report describes an acoustic detector for passive acoustic monitoring of ocean data. The detector is described and its theoretical performance outlined in view of practical implementation on board the SUBECO buoys. The detector is preliminary tested on a data set collected during the May 2019 bouy deployment off the coast of Portugal.
Clearance	UNCLASSIFIED
Distribution list	CINTAL (1), SiPLAB(1), IH(1)
Total no. copies	3 (three)

Approved for publication

A.E.B. Ruano

President of the Administration Board

Contents

List of Figures

Abstract

This report describes a simple acoustic energy detector for passive acoustic monitoring of ocean data. The detector is sufficiently simple, yet efficient, to be implemented on real time. The detector is presented and its theoretical performance outlined in view of practical implementation on board the SUBECO buoys. In particular, a strategy based upon percentiles is proposed for robust noise estimation on noise records contaminated with high energetic ship noise. The detector is preliminary tested on two days of data collected during the April - May 2019 bouy deployment off the coast of Portugal.

(intentionally blank)

Chapter 1

Introduction

In theory and generally speaking, event detection requires the knowledge of the waveform to be detected or "you can only find if you know what you are looking for". In practice the problem is not that simple since random effects create a zone of uncertainty where detection becomes a statistical problem.

Uncertainty may appear at least at two levels: the emitted signal waveform may not be completely known or even unknown, or the propagation of the signal between the emission point and the receiver may introduce randomness on signal arrival, amplitude, phase, frequency and waveform in general. Other source of uncertainty is, of course, observation noise that is generally assumed additive and non-correlated with the signal. This problem was dealt with and demonstrated in a realistic shipping noise field based on a numerical propagation model derived from real environmental temperature profiles and Automatic Information System (AIS) data off the coast of Portugal [1].

General theory casts this problem under the class of hypothesis testing where an observation-based statistic is tested against a given threshold. The statistic is based on the signal to be detected (or on the *a priori* knowledge we may have of it) and the threshold is based on (assumed) noise statistics and a chosen false alarm rate. In other words: in order to define a detector we have to make assumptions about the signal and about the noise.

The most basic assumption is: we don't know anything about the signal nor the noise. We don't know which signal we are looking for: its duration, amplitude, frequency content or time of arrival. We also don't know when the signal is present and when it is not, so it becomes difficult to estimate the noise statistics, since it can be corrupted by the signal.

This is a situation often encountered and since the signal is unknown it should be considered as random. The channel free detector in that case is the so-called energy detector if the signal is random and white (uncorrelated). If the signal is random but not white (correlated) and the correlation is known, the correlation can be used in the so-called estimator-correlator detector setup. The performance of both detectors can be equated in a very simple manner if the observation noise is assumed uncorrelated and Gaussian distributed. Another question is how to actually implement the detector, which requires some knowledge of the noise statistics for deriving a workable threshold.

Of course extensive supervised testing of the detector against real data is the ultimate step before practical application. In the SUBECO setting this supposes that the detector is relatively simple and robust to be embedded on the embarked electronics. In this

report a limited test is performed on two days of data recorded in May 2019, during a test deployment off the west coast of Portugal.

This report si organized as follows: the developed methods and required background are recalled in section 2, including the detector statistics and the expected theoretical performance both for the stationnary noise energy detector in section 2.1.1 and for the non-wide sense stationnary case in section 2.1.2. The problem of noise variance estimation is examined in section 2.2, focusing on the percentile method, supported by an example (section 2.2.2) and implementation suggestion (section 2.2.3). Kurtosis, section 2.2.4, is also recalled as a possible alternative for noise variance estimation. The testing on the SUBECO data set is presented in section 3, and conclusions are drawn in section 4.

Chapter 2

Methods and background

2.1 Detector statistics

The observed signal model is given by

$$\mathbf{y} = \mathbf{x} + \mathbf{w} \tag{2.1}$$

where $\mathbf{y}^T = [y_0, y_1, \ldots, y_{N-1}]$ is a vector with the observed time samples y_n, obtained at a given sampling rate $T_s \leq 2/f_m$ s, where f_m is the maximum frequency contained in the signal; $\mathbf{x}$ and $\mathbf{w}$ contain the samples of the signal and the noise processes, respectively; N is the discrete observation window size. In this setting the noise vector in the time window of N samples is assumed to be zero-mean, white and Gaussian distributed so $\mathbf{w} : \mathcal{N}[\mathbf{0}, \mathbf{C}_w]$. In general if the noise is assumed as wide-sense stationnary (WSS) then $\mathbf{C}_w = \sigma^2\mathbf{I}$, if not $\mathbf{C}_w = \text{diag}(\sigma_0^2, \sigma_1^2, \ldots, \sigma_{N-1}^2)$.

Briefly speaking in the simple binary hypothesis testing case, if the signal is deterministic the optimal statistic is given by the Neyman-Pearson (NP) detector that accepts hypothesis H_1 that a signal is present if

$$T_d[\mathbf{y}] = \mathbf{y}^t\mathbf{C}_w^{-1}\mathbf{x} > \gamma, \tag{2.2}$$

where γ is some *a priori* threshold. If the signal $\mathbf{x}$ is assumed random, zero-mean, Gaussian and uncorrelated with the noise, such that $\mathbf{x} : \mathcal{N}[\mathbf{0}, \mathbf{C}_x]$, the optimal NP statistic accepts H_1 if

$$T_r[\mathbf{y}] = \mathbf{y}^t[\mathbf{C}_w^{-1}(\mathbf{C}_x^{-1} + \mathbf{C}_w^{-1})^{-1}]\mathbf{y} > \gamma. \tag{2.3}$$

Case (2.2) is known as the correlator-detector, since it picks the output of a matched-filter correlator with the known signal at sample $N-1$. Case (2.3) is known in the literature as the estimator-correlator, since an estimate $\hat{\mathbf{x}}$ of random signal $\mathbf{x}$ is obtained as

$$\hat{\mathbf{x}} = [\mathbf{C}_w^{-1}(\mathbf{C}_x^{-1} + \mathbf{C}_w^{-1})^{-1}]\mathbf{y}, \tag{2.4}$$

before correlating with the observation $\mathbf{y}$. Relation (2.4) is also known as the Wiener filter output estimate. The simplest case is when the middle matrix in (2.3) is identity or diagonal which leads to a statistic proportional to $|\mathbf{y}|^2$ also known as the energy detector.

2.1.1 The wide-sense stationnary energy detector

The energy detector derives from the case of the random white signal in white noise, where $\mathbf{C}_x = \sigma_x^2\mathbf{I}$ and $\mathbf{C}_w = \sigma^2\mathbf{I}$. In this trivial case (2.3) reduces to

$$T_r[\mathbf{y}] = \frac{\sigma_x^2/\sigma^2}{\sigma_x^2+\sigma^2}\sum_{n=0}^{N-1}|y(n)|^2 > \gamma, \tag{2.5}$$

or equivalently

$$T_r[\mathbf{y}] = \sum_{n=0}^{N-1}|y(n)|^2 > \gamma'. \tag{2.6}$$

Since $y(n)$ is zero mean Gaussian distributed with variance σ^2 and $\sigma^2+\sigma_x^2$, under H_0 and H_1, respectively, we can say that

$$\frac{Tr[\mathbf{y}/H_0]}{\sigma^2} \;:\; \chi_N^2, \tag{2.7}$$

$$\frac{Tr[\mathbf{y}/H_1]}{\sigma_x^2+\sigma^2} \;:\; \chi_N^2, \tag{2.8}$$

where the χ^2 random distribution with N degrees of freedom results from the summation of N independent standard χ^2 random variables. If the number of samples N is larger than, say, 30, χ_N^2 tends to a Gaussian distribution.

In this case, the probabilities of false alarm and detection are

$$\begin{aligned} P_{FA} &= \text{Prob}[Tr(\mathbf{y}/H_0) > \gamma], \\ P_D &= \text{Prob}[Tr(\mathbf{y}/H_1) > \gamma], \end{aligned}$$

respectively, or with the Gaussian assumption and using (2.7) and (2.8),

$$\begin{aligned} P_{FA} &= 1 - \text{Prob}[Tr(\mathbf{y}/H_0) \le \gamma], \\ &= 1 - \text{Prob}\left[\frac{Tr(\mathbf{y}/H_0)}{\sigma^2} \le \frac{\gamma}{\sigma^2}\right], \\ &= Q_{\chi_N^2}\left(\frac{\gamma}{\sigma^2}\right), \end{aligned} \tag{2.9}$$

$$\begin{aligned} P_D &= 1 - \text{Prob}[Tr(\mathbf{y}/H_1) \le \gamma], \\ &= 1 - \text{Prob}\left[\frac{Tr(\mathbf{y}/H_0)}{\sigma_x^2+\sigma^2} \le \frac{\gamma}{\sigma_x^2+\sigma^2}\right], \\ &= Q_{\chi_N^2}\left(\frac{\gamma}{\sigma_x^2+\sigma^2}\right), \end{aligned} \tag{2.10}$$

where $Q_{\chi_N^2}$ is the tail distribution function for the χ_N^2 variable. From (2.9),

$$\frac{\gamma}{\sigma^2} = Q_{\chi_N^2}^{-1}(P_{FA}), \tag{2.11}$$

where $Q_{\chi_N^2}^{-1}$ is the Q function inverse. Plugging (2.11) into (2.10) gives

$$P_D = Q_{\chi_N^2}\left[\frac{Q_{\chi_N^2}^{-1}(P_{FA})}{1+\rho}\right], \tag{2.12}$$

where ρ is the signal to noise ratio (SNR) defined as $\rho = \sigma_x^2/\sigma^2$.

This last equation is represented in figure 2.1 as a function of SNR (in dB) for given values of P_{FA} (a) and as function of P_{FA} for given values of SNR (b) - the so called Receiver Operating Caracteristic (ROC). The SNR in dB is defined as

$$\begin{aligned} SNR_{\text{dB}} &= 10\log_{10}\left(\frac{\sigma_x^2}{\sigma^2}\right), \\ &= 10\log_{10}\rho. \end{aligned} \tag{2.13}$$

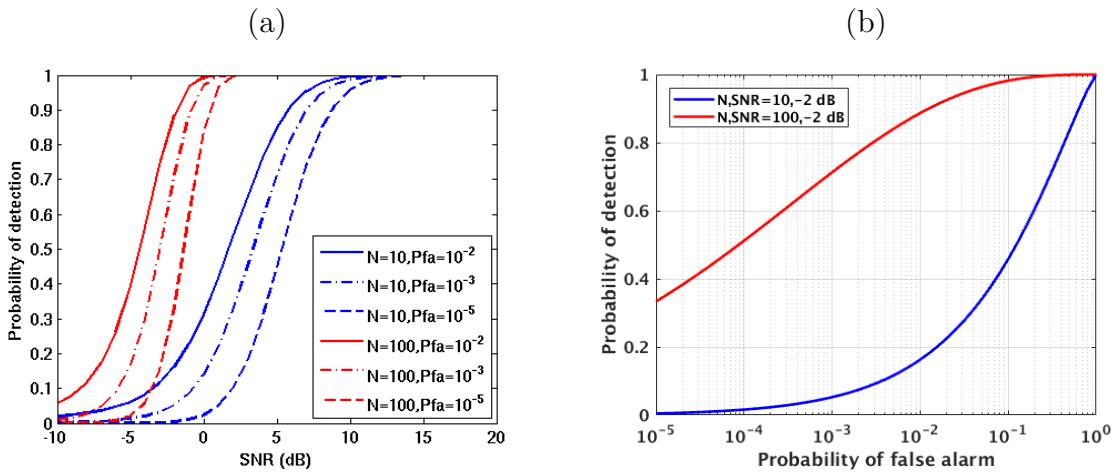

Figure 2.1: energy detector for the zero mean white Gaussian stationnary noise case: probability of detection versus SNR (a) and receiver operating characteristic (ROC) (b).

2.1.2 The non-stationnary energy detector

In the case of non-WSS noise (but still zero mean, white and Gaussian) we may have $\mathbf{C}_w = \text{diag}(\sigma^2(0), \sigma^2(1), \ldots, \sigma^2(N-1))$ which indicates that the noise power varies along the horizon of observation of N samples. In order to determine the performance of the energy detector, it requires a new definition of SNR where ρ in (2.13) is replaced by the mean

$$\bar{\rho} = \frac{1}{N}\sum_{n=0}^{N-1}\rho(n), \tag{2.14}$$

where $\rho(n) = \sigma_x^2/\sigma^2(n)$ is the instantaneous SNR at time sample n.

The test statistic (2.5) for this non-WSS case may be written

$$T_r[\mathbf{y}] = \sum_{n=0}^{N-1}\frac{\sigma_x^2}{\sigma^2(n)[\sigma_x^2+\sigma^2(n)]}|y(n)|^2 \tag{2.15}$$

or under the two hypothesis

$$T_r[\mathbf{y}/H_0] = \sum_{n=0}^{N-1}\frac{\sigma_x^2}{\sigma_x^2+\sigma^2(n)}\left|\frac{w(n)}{\sigma(n)}\right|^2,$$

$$= \sum_{n=0}^{N-1} \frac{\rho(n)}{1+\rho(n)} \left|\frac{w(n)}{\sigma(n)}\right|^2, \tag{2.16}$$

$$T_r[\mathbf{y}/H_1] = \sum_{n=0}^{N-1} \frac{\sigma_x^2}{\sigma^2(n)} \left|\frac{y(n)}{\sqrt{\sigma_x^2+\sigma^2(n)}}\right|^2$$

$$= \sum_{n=0}^{N-1} \rho(n) \left|\frac{x(n)+w(n)}{\sqrt{\sigma_x^2+\sigma^2(n)}},\right|^2, \tag{2.17}$$

As above, the two quantities in $|\ |$ are standard χ^2 distributed variables, but they result in a weighted sum as

$$T_r[\mathbf{y}/H_0] = \sum_{n=0}^{N-1} \frac{\rho(n)}{1+\rho(n)}\chi^2, \tag{2.18}$$

$$T_r[\mathbf{y}/H_1] = \sum_{n=0}^{N-1} \rho(n)\chi^2, \tag{2.19}$$

These weighted summations of χ^2 variables, give raise to a random variable which distribution is not known analitically and has to be approached numerically. One way to do this is by using the `qf` algorithm proposed by Davies [2] which gives an estimate of the distribution of a weighted sum of χ^2 standard independent variables. So, using the same procedure as above, we can write the probability of detection P_D as a function of the probability of false alarm P_{FA} as

$$P_D = 1 - H_{\chi_N^2}[G^{-1}_{\chi_N^2}(1-P_{FA})] \tag{2.20}$$

where $G_{\chi_N^2}(\nu)$ and $H_{\chi_N^2}(\nu)$ are the cumulative distribution functions numerically evaluated using the `qf` algorithm for the variables (2.18) and (2.19), respectively, and $G^{-1}_{\chi_N^2}(\nu)$ the inverse of $G_{\chi_N^2}$.

In order to derive the performance of the energy detector in this non-WSS case, we need to define matrix $\mathbf{C}_w$ or, the non-stationnary evolution of the noise power along time. As an example we may consider that the noise power fluctuates between a minimum and maximum value according to a uniform distribution. Thus, the random variable Z associated with $\rho(n)$ will be distributed as $Z : \mathcal{U}[a,b]$, where a and b are the lower and upper bounds of the uniform probability density function. For this example we have set $a = \bar{\rho} - 0.5\bar{\rho}$ and $b = \bar{\rho} + 0.5\bar{\rho}$, where $\bar{\rho}$ is the requested SNR. It can be easily seen that the interval $[a,b]$ narrows as the SNR decreases and that the mean is $m_Z = (a+b)/2 = \bar{\rho}$ and the standard deviation is $\sigma_Z = \bar{\rho}/\sqrt{12} = 0.288\bar{\rho}$.

The resulting performance curves are shown in figure 2.2 for the same intervals and within the same bounds as for figure 2.1. The performance is slightly worst than that of the stationary noise case with small wrinkles due to difficulty to choose the sampling interval for the numerical evaluation of the `qf` function and then computing the inverse of $G_{\chi^2}(\nu)$.

2.2 Determining noise variance

In order to practically implement (2.6) the threshold γ needs to be defined. Using (2.11) the threshold is given by

$$\gamma = \sigma^2 Q^{-1}_{\chi_N^2}(P_{FA}) \tag{2.21}$$

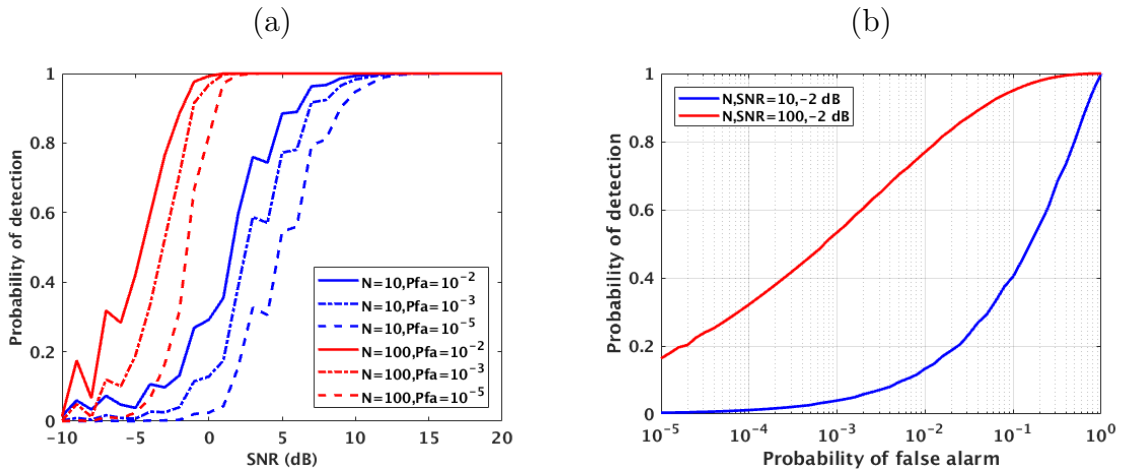

Figure 2.2: energy detector for the zero mean white Gaussian non stationnary noise case: probability of detection versus SNR (a) and receiver operationg characteristic (ROC) (b).

which requires fixing a certain expected probability of false alarm and the knowledge of the noise variance σ^2, which needs to be estimated from the actual data.

Estimating noise variance is not always easy since it requires producing a statistic of the noise only and also because this needs to be done (or updated) through time in order to adapt to changing background noise levels (thus the previous performance study for the non-WSS case).

2.2.1 The percentile method

A well known method for estimating the variance is the p-percentile of the, assumed known, sample distribution.

The p-percentile is the value under which p percent of the population falls. If the sample size N is sufficiently large, determining an estimate of the p-percentile is equivalent to determining the value of the sorted sequence of variables for the p percent of the sample size. In other words if $u_i; i = 1, \ldots, N$ is the ensemble of draws of the random variable U with cumulative distribution function $F_U(u)$, and $\mathbf{U}$ is a vector with the N sorted draws such that

$$\mathbf{U} = \{u_1 \leq u_2 \leq \ldots, u_k, \leq \ldots, u_N\} \tag{2.22}$$

then the p-percentile is $u(p) = u_{I(p;N)}$, where $I(p; N)$ is given by

$$I(p; N) = 100\left(\frac{p - 0.5}{N}\right), \qquad p = 1, 2, \ldots, N \tag{2.23}$$

and then we can approximate $(p/100) = F_U[u(p)]$. If $F_U(u)$ is a known function of the variance it allows for its estimation. Since the time interval with the N random samples may contain signal and noise, care should be taken to chose a low percentile p, say, $10 \leq p \leq 20$ % so as to avoid the signal part (that is supposed to have a higher energy than the noise) and take only the noise samples due to the sorting. In practice the p-percentile is implemented using the Matlab function `prctile(X,p)`, where X is the ensemble of random samples.

2.2.2 Example

Let us take the case of a χ^2 distributed random variable of order 2. According to appendix A its cdf is given by

$$F_Z(z) = 1 - e^{-z/\sigma_z} u(z). \tag{2.24}$$

making now

$$\frac{p}{100} = 1 - e^{-u(p)/\sigma_z} \tag{2.25}$$

we get

$$\sigma_z = -\frac{u(p)}{\log(1 - p/100)} \tag{2.26}$$

which then leads to the noise variance $\sigma_w^2 = \sigma_z/2$.

Figure 2.3 shows an example for an order $k = 2$ and $\sigma_w = 3$ where the procedure is as follows :

1. two N-sample independent Gaussian distributed random variables X_1 and X_2 with standard deviation σ_w are generated;
2. a N-sample χ_2^2 random variable Y is calculated as $Y = X_1^2 + X_2^2$;
3. the standard deviation of Y is estimated using the `std` routine of Matlab and the p-percentile method using (2.26)
4. this is repeated for 20 draws and means estimated

As expected the estimated standard deviation of Y tends to $2\sigma_w^2$ as N increases. For low N `std` tends to underestimate the standard deviation while the p-percentile tends to overestimate it.

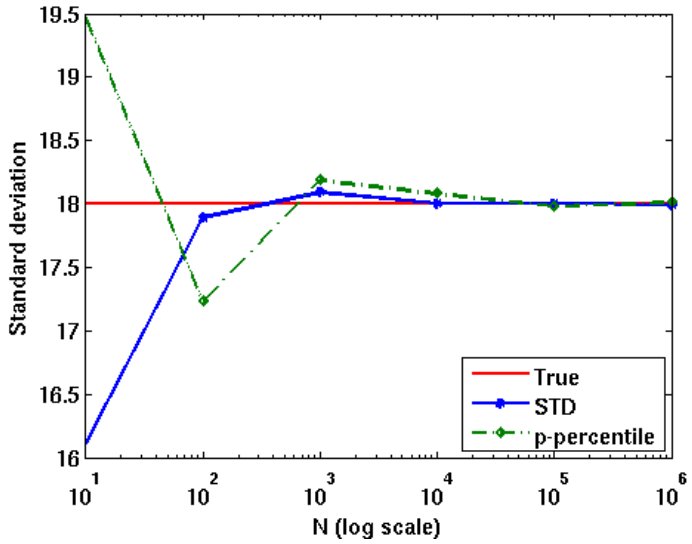

Figure 2.3: standard deviation estimate for a χ_2^2 with standard deviation of 18 with std function of Matlab (blue) and using the p-percentile method (green) for a sample size N from 10 to 1000000. The curves result from 20 independent draws.

2.2.3 Implementation

For band-pass signals the power is replaced by the power of the envelope. That is

$$p_y(t) = y_p^2(t) + y_q^2(t) \tag{2.27}$$

where $y_p(t)$ and $y_q(t)$ are the in phase and quadrature low pass components of signal $y(t)$ down heterodined by the center frequency of the frequency band. If signal $y(t)$ is filtered in the band $B : [f_1, f_2]$, then $f_c = (f_1 + f_2)/2$.

So, if the sampled version $y(n)$ of $y(t)$ is a sequence of Normal distributed random variables, $p(n)$ will be χ_2^2 and the previously described p-percentile procedure applies for $k = 2$.

2.2.4 Using Kurtosis

Kurtosis has been first proposed by Karl Pearson and is based on a scaled version of the fourth of a population sample[1]. The fourth moment is associated with the "tailedness" of a distribution (in a similar way as "skewness"). Higher kurtosis is the result of infrequent extreme deviations (or outliers), as opposed to frequent modestly sized deviations. An univariate Normal distribution has a kurtosis of 3. Sometimes the excess kurtosis $\eta = \kappa - 3$ is used.

The definition is then

$$\begin{aligned} \kappa[X] &= E\left[\left(\frac{X-\mu}{\sigma}\right)^4\right], \\ &= \frac{\mu_4}{\sigma^4}, \\ &= \frac{E[(X-\mu)^4]}{(E[(X-\mu)^2])^2}, \end{aligned} \tag{2.28}$$

The interpretation of Kurtosis is sometimes controversial, where some authors wrongly describe kurtosis as a measure of "peakedness" of the distribution while others correctly relate it to the "tailedness" of the distribution, or to a measure of "outliers". Kurtosis has been widely used for detection and classification of non-Gaussian signals in Gaussian noise. Using Kurtosis as the sole criteria for that purpose may introduce strong flaws, but used in conjunction with other measures may help in detection purposes.

In particular Kurtosis may be used to detect snapshots strongly contaminated with signal and thus help adjusting the p-percentile for noise estimation in those snapshots.

For instance one could determine the mean variance estimate over K snapshots as

$$\bar{\sigma}(K) = \frac{1}{K}\sum_{k=1}^{K}\hat{\sigma}(k) \tag{2.29}$$

that can be obtained sequentially as

$$\bar{\sigma}(K) = \frac{\hat{\sigma}(K)}{K} + \frac{K-1}{K}\bar{\sigma}(K-1). \tag{2.30}$$

[1] see `https://en.wikipedia.org/wiki/Kurtosis`.

If a forgetting factor K_0 is introduced,

$$\bar{\sigma}'(K) = \frac{1}{K}\sum_{k=1}^{K}\hat{\sigma}(k)e^{-(K-k)/K_0} \tag{2.31}$$

or again sequentially,

$$\bar{\sigma}'(K) = \frac{\hat{\sigma}(K)}{K} + \frac{(K-1)e^{-1/K_0}}{K}\bar{\sigma}'(K-1). \tag{2.32}$$

where the value of the forgetting factor K_0 may be associated with the Kurtosis κ of the distribution given by (2.28).

Chapter 3

The SUBECO test data

The SUBECO buoy was deployed on a deep water area off the west coast of Portugal from mid April to mid May, 2019. Figure 3.1(a) shows an artistic drawing of a SUBECO buoy (not to scale) with the acoustic array formed by six broadband hydrophones at the vertices of a tetrahedron of 1.5 m side, deployed at approximately 80 m depth. The acquired data is cabled to the surface buoy allowing for remote status monitoring, data inspection through a remote satellite link and storage. Figure 3.1(b) shows the deployment location. The selected location has a water depth of approximately 1300 m and is in the vicinity of the shipping Trafic Separation System (TSS) shown in the background as historical ship density drawn from AIS data[3].

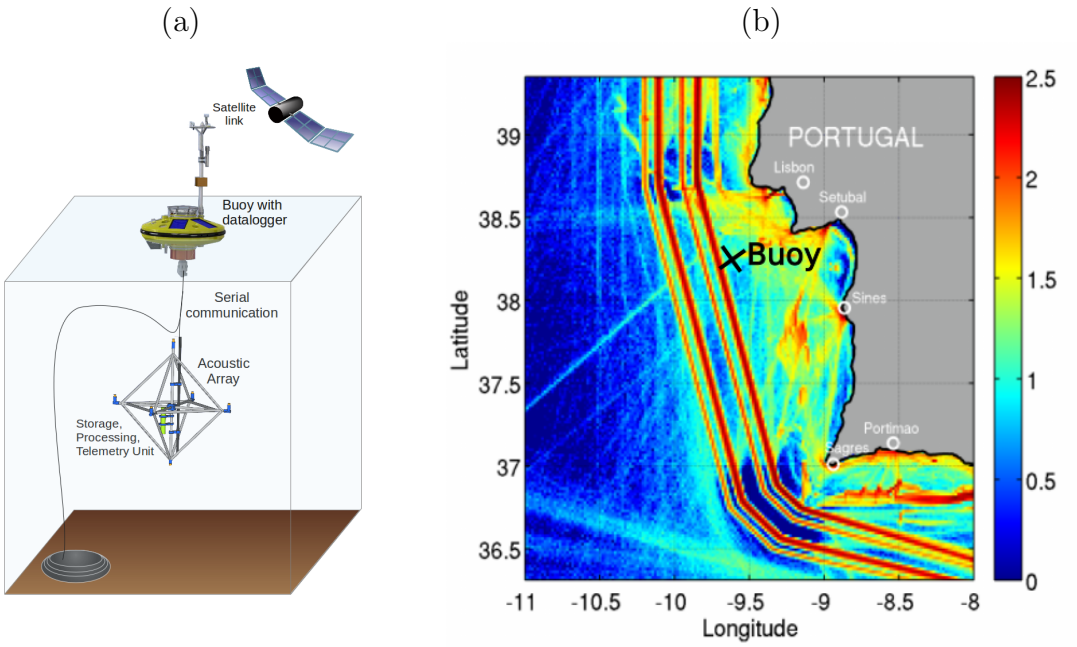

Figure 3.1: *SUBECO buoy experiment and data: artistic drawing (a), AIS ship density map with buoy deployment location from mid April to mid May, 2019 (b).*

3.1 Non-acoustic data

The primary scope of the SUBECO buoy is to acquire meteorological and environmental data for weather and sea status operational analysis. This data was not made avalilable for the period at hand.

Another non-acoustic data set concerns the positioning in depth, tilt and rotation of the acoustic receiving tetrahedron array. This is provided by a set of sensors that allow to determine depth, heading, pitch and roll but are only needed for the spatial coherent processing of the hydrophone array as a whole, so they are not described here.

3.2 Acoustic data

3.2.1 Hydrophone setup

The hydrophone used is from Sensor Technology Ltd, model SQ-26. Its main characteristics are summarized in table 3.1.

Parameter	unit	value
depth rating	m	2000
sensitivity	dB//1V/μPa	-193
bandwidth	kHz	0.001-28

Table 3.1: Sensor Technology Ltd, hydrophone SQ-26 main characteristics.

The frequency response of the hydrophone was not provided, so it was assumed flat in the useful frequency band (up to $f_s/2$). Gain and sensitivities are known through a `csv` file written by the data acquisition firmware so, an approximate calibration of sound pressure level at the hydrophone input is possible.

3.2.2 Acoustic recording

The data acquisition duty cycle is 1/6, corresponding to 100 s worth of data every 10 min: 60 s where obtained at a sampling rate of 10 kHz, 30 s at 50 kHz and 10 s at 100 kHz.

Approximately two days worth of data, from May 5, 15:25 to May 7, 07:15 (UTC), were handed to us for testing purpose on two sampling frequency sets: 10 and 50 kHz, termed as LF and HF, respectively. The PSD estimates over 60 s for the LF set and 30 s for the HF set, are shown in figures 3.2(a) and (b), respectively. Averaging over each data ping destroys most of the short term signal structure but reveals long trend features such as numerous broadband spikes reaching, in many occasions, the whole 25 kHz band. The low frequency band noise has a notoriously high level with long traces of tonal frequencies below 500 Hz (a). These tones may be difficult to detect by algorithms designed for impulsive noise. Although no traces of biological noise can be seen in these figures, a closer look reveals several files with (most certainly) dolphin vocalizations, an example of which is shown in Fig. 3.3(a) while a possible ship component is shown in (b).

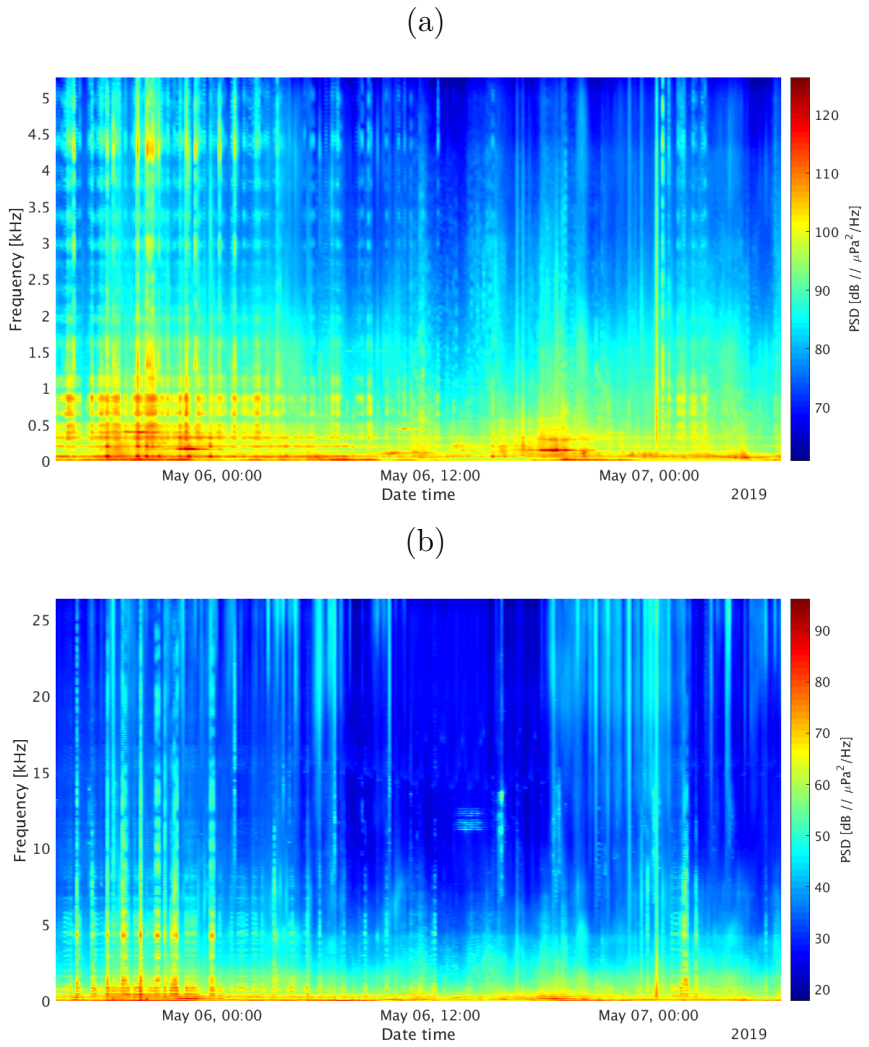

Figure 3.2: sample PSD of received signal on hydrophone 1 for sampling frequency f_s 10 kHz (a) and 50 kHz (b).

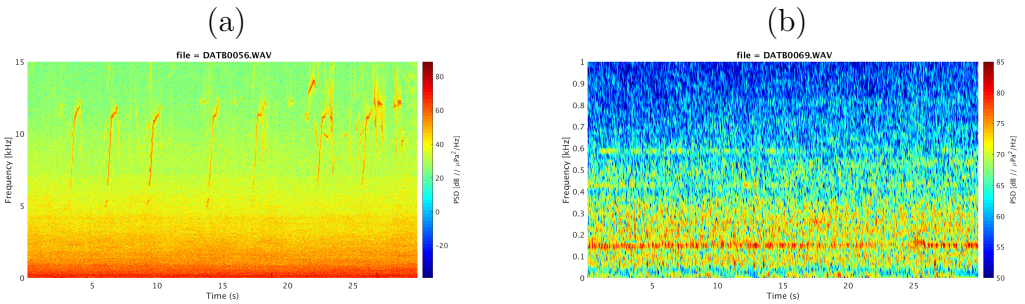

Figure 3.3: examples of marine mammals vocalization (a) and a possible ship tonal component (b).

3.2.3 Event detection

The (mostly) ambient noise periods of each record over the two days of recording were used to test (and train) an automatic event detector / analyser. The recordings were

filtered through three frequency bands: [100 Hz - 1.5 kHz] believed to be dominated mostly by shipping noise, [1.5 - 8 Khz] mostly associated with biological and surface noise and [$\geq$ 8 kHz] a decreasing noise level region where biological and bubble noise prevails (according to Wenz). The detector was run separately on each band.

Then, the p-percentile strategy described in section 2.2 was applied to estimate the noise variance and set as an event detector to be run independently on each time record and frequency band. A percentile $p = 20\%$ and a $P_{FA} = 0.001$ were selected throughout the data set and for the three bands. Figure 3.4 shows the results obtained for the percentage of detections (a) and for the estimated detection duration (in seconds) (b).

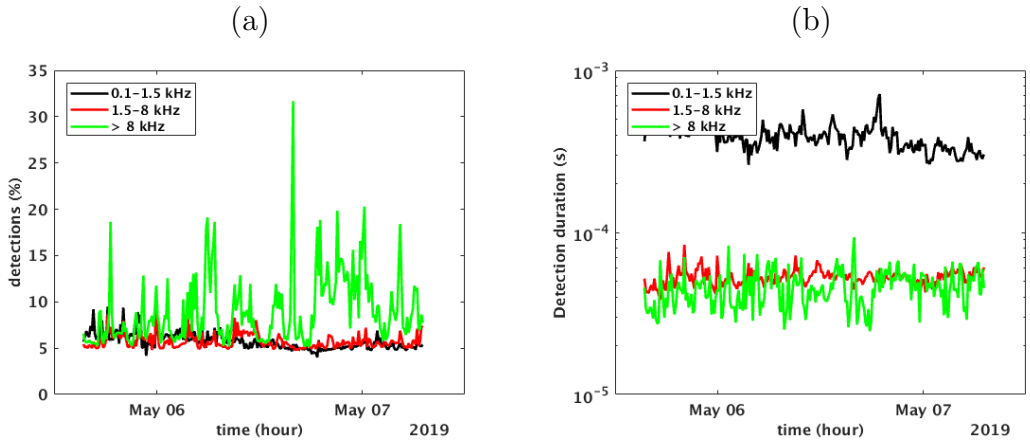

Figure 3.4: event detection results from May 5 15:25 to May 7 07:15, 2019 per 30 s time record at 50 kHz sampling rate: raw detection percentage (a) and detected interval duration (in s) (b).

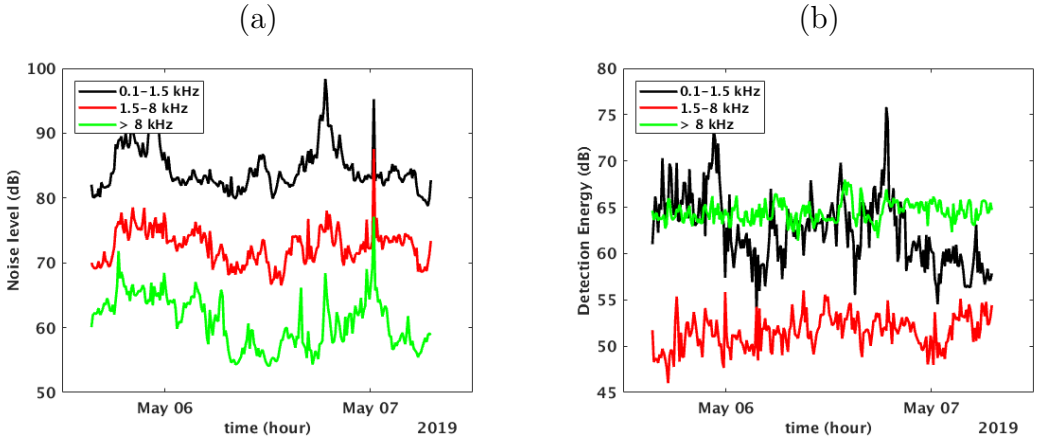

Figure 3.5: event detection results from May 5 15:25 to May 7 07:15, 2019 per 30 s time record at 50 kHz sampling rate: background noise level (a) and detection energy (b).

As expected the base detections' count on Figure 3.4(a) varies between 5 and 8% of the total number of samples on each record (which is set to 1.5 10^6) for the lower and mid band while it largely exceeds those numbers reaching up to 30% for the high-frequency band, with a somewhat larger % in the second half of the observation period. Of course the detection duration, which is the mean duration of all detected signals over a record

of 30 s, is anti-proportional to the frequency band, reaching as low as one sample for the band above 8 kHz, and much larger values for the band below 1.5 kHz.

The noise level background and detected energy are shown in Figure 3.5(a) and (b), respectively.

The noise background level corresponds to the mean estimated noise variance (in dB) over each 30 s interval, and varies also anti-proportional to the frequency band. Instead, the total detected energy which is the total power summed between two up and down crossings of the detection threshold multiplied by the interval duration showed, in figure 3.5(b), some correlation with the background noise level curve of figure 3.5(a) with highly variable energies in the low-frequency band and a low variability for the mid and high bands.

Chapter 4

Conclusions

This report aimed at deriving, implementing and testing a simple acoustic event detector adapted to ocean data recovered from an offshore surveillance buoy. The buoy is serviced approximately every six month so the recovered data set may be very large and the detector is expected to relatively quickly cope with such amount of data. Eventually, the detector may be adapted to be embedded on the buoy acquisition software and run on the fly directly on the online data.

In the first section the energy detector is proposed and its theoretical performance described both for the stationary and non-stationary noise cases. A simple procedure for determining noise variance is proposed and its performance tested on simulation.

Finally, the detector is run on a data sample of two days worth of data obtained by the SUBECO buoy off the west coast of Portugal on May 6-7, 2019. These are preliminary results that due to lack of time could not be detailed for individual data intervals and linked with meaningful signals such as ships or marine mammal calls. Further investigation would be needed in that case.

Bibliography

[1] S.M. Jesus. Passive target detection in ais modeled shipping noise off the west coast of portugal. Report CINTAL-6/17, CINTAL, Universidade do Algarve, Faro (Portugal), October 2017.

[2] R.B. Davies. The distribution of a linear combination of χ^2 random variables. *Applied Statistics*, 29:323–333, 1980.

[3] C. Soares, F. Zabel, and S.M. Jesus. A shipping noise prediction tool. In IEEE, editor, *Proc. of MTS/IEEE Oceans'15*, Genova, Italy, May 2015.

Appendices

A Generalized χ^2 variables of order 1 and 2

A.1 The standard case

Let us consider the standard Gaussian variable $X : \mathcal{N}[0, 1]$. The χ^2_1 variable $Y = X^2$ of order $k = 1$ has the following probability density function (pdf)

$$f_Y(y) = \frac{1}{\sqrt{2\pi y}} e^{-y/2} u(y), \tag{A.1}$$

where $u(y)$ is the unit step function. The corresponding cumulative distribution function (cdf) is therefore given by

$$F_Y(y) = \int_0^y \frac{1}{\sqrt{2\pi t}} e^{-t/2} dt, \tag{A.2}$$

which has no closed form solution.

If now we have two standard and independent Gaussian variables X_1 and X_2 the χ^2_2 variable $Y = X_1^2 + X_2^2$ of order $k = 2$ will have the following pdf

$$f_Y(y) = \frac{1}{2} e^{-y/2} u(y), \tag{A.3}$$

that allows for a closed form cdf (always available when the order k is even)

$$F_Y(y) = 1 - e^{-y/2} u(y). \tag{A.4}$$

For all k we will have the mean $\mu = k$ and the variance $\sigma^2 = 2k$.

A.2 The generalized case

Let us now turn to the generalized case where the random Gaussian variables are still zero mean, but have a variance σ_x^2 different from one. Thus, in the case of order one $\tilde{X} : \mathcal{N}[0, \sigma_x]$, the question is what are the pdf and cdf for the variable $Z = \tilde{X}^2$?

Obviously, if we make the change of variable $X = \tilde{X}/\sigma_x$, then X will be standard Gaussian and what was said before will apply. So, by making the change of variable in Z, let's find out the distribution of $Z = \sigma_x^2 X^2 = \sigma_x^2 Y$ where Y is the standard χ^2_1 variable.

Let's start with the cdf of Z

$$F_Z(z) = Prob[Z \leq z] = Prob[\sigma_x^2 Y \leq z] = Prob[Y \leq \frac{z}{\sigma_x^2}] = F_Y\left(\frac{z}{\sigma_x^2}\right), \tag{A.5}$$

and therefore by using (A.2)

$$F_Z(z) = \int_0^{z/\sigma_x^2} \frac{\sigma_x}{\sqrt{2\pi t}} e^{-t/(2\sigma_x^2)} dt, \tag{A.6}$$

which, again, has no closed form solution.

Its pdf is obtained either be differentiating $F_Z(z)$ or by knowing that the change of variable on the pdf produces

$$\begin{aligned} f_Z(z) &= \frac{1}{\sigma_x^2} \frac{1}{\sqrt{2\pi z/\sigma_x^2}} e^{-z/2\sigma_x^2} u(z), \\ &= \frac{1}{\sigma_x \sqrt{2\pi z}} e^{-z/(2\sigma_x^2)} u(z). \end{aligned} \tag{A.7}$$

If we turn to the order 2, we will consider two non standard Gaussian variables $\tilde{X}_1$ and $\tilde{X}_2$ with same variance $\sigma_x^2 \neq 1$, thus the generalized χ_2^2 variable $Z = X_1^2 + X_2^2$ may be written through the change of variable $Z = \sigma_x^2 Y$ where the pdf and cdf of Y are given by (A.3) and (A.4), respectiely. Making the change of variable for the cdf as in (A.5) using (A.4) one can write

$$F_Z(z) = 1 - e^{-z/2\sigma_x^2} u(z). \tag{A.8}$$

and for the pdf

$$f_Z(z) = \frac{1}{2\sigma_x^2} e^{-z/2\sigma_x^2} u(z). \tag{A.9}$$

It is easy to demonstrate that for $k = 2$, the mean is $\mu_Z = 2\sigma_x^2$ and the variance is $\sigma_Z^2 = 4\sigma_x^4$. Using this expression of the variance of Z we can write the pdf and cdf of Z as

$$F_Z(z) = 1 - e^{-z/\sigma_z} u(z). \tag{A.10}$$

and

$$f_Z(z) = \frac{1}{\sigma_z} e^{-z/\sigma_z} u(z), \tag{A.11}$$

respectively.